Available online at www.sciencedirect.com
ScienceDirect
Ceramics International 35 (2009) 3401–3406
CERAMICS INTERNATIONAL
www.elsevier.com/locate/ceramint

# Structural, optical and bioactive properties of calcium borosilicate glasses

K. Singh *, Indu Bala, Vishal Kumar

*School of Physics and Materials and Science, Thapar University, Patiala 147004, India*

Received 17 January 2009; received in revised form 8 May 2009; accepted 10 June 2009
Available online 7 July 2009

**Abstract**

Glass of composition $40SiO_2$–$20B_2O_3$–$30CaO$–$10M_2O_3$ (M = Al, Cr, Y and La) were prepared by the splat quenching technique to investigate the effect of $M_2O_3$ on their bioactivity, structural and optical properties. $Y_2O_3$ and $Cr_2O_3$ containing glasses formed a crystalline hydroxyapatite (HA) layer after dipping in simulating body fluid (SBF) for 25 days. On the other hand, HA layer could not form in $Al_2O_3$ and $La_2O_3$ glasses. However, during soaking in SBF solution, these glasses exhibit higher dissolution rate, lower density and increased optical band gap as compared to unsoaked glasses. Their oxygen molar volume was also higher than for $Y_2O_3$ and $Cr_2O_3$ glasses. The change in composition affects the cross-link formation in the glass matrix and finally its durability and bioactivity in SBF. The results show that $M_2O_3$ plays an important role in controlling chemical durability and bioactivity of the glasses.


*Keywords:* D. Glass; D. Silicate; E. Biomedical applications; Hydroxyapatite

## 1. Introduction

Bioactive glass and glass ceramics are suitable bone bonding materials [1,2]. They form a fast direct bond with bone defects. However, formation of a bond with the apatite layer depends upon initial glass composition, its volume and processing conditions [3]. Hench et al. [1] have reported that the bonding of bioactive glass and glass ceramics to bone tissue is associated with a series of chemical interactions between surrounding fluids and tissue. In this process, initially a silicon rich layer is formed on the glass surface, followed by the formation of a calcium phosphate rich layer [2]. The bioactive behaviour of glasses was reported for the first time by Hench [1,4] in $P_2O_5$–$SiO_2$ glass. Kokubo [5] and Oktsuki et al. [6] demonstrated that phosphate free calcium silicate glass also formed the apatite layer when the glass was exposed to a simulated body fluid for 2–30 days. Ryu et al. [7] also showed bioactivity in the CaO–$SiO_2$–$B_2O_3$ glass system. The additions of intermediate oxide in glass composition influence the properties of the glasses due to their possible existence in different oxidation states. For instance 5 mol.% of $Al_2O_3$ acts as a network former. Nevertheless, above this percentage it works as network modifier in MgO-based glasses [8]. Additionally, high molecular weight of intermediate oxide improves the mechanical properties of the glasses without affecting their bioactivity [9]. Doping of ZnO in phosphate glass also improves cell attachment [10]. On the other hand, slow accumulation of metal ions such as chromium may lead to adverse clinical reactions. However, chromium based alloys have been used in joint arthoplasty due to their good load bearing properties with excellent wear resistance [11]. Schwickert et al. [12] reported addition of $La_2O_3$ and $Y_2O_3$ to increase the mechanical strength and melting point of the glasses whereas $Cr_2O_3$ and $Al_2O_3$ reduce their surface tension.

The objective of the present study is to synthesize $40SiO_2$–$20B_2O_3$–$30CaO$–$10M_2O_3$ bioactive glasses and study the effect of $M_2O_3$ (M = Al, Cr, Y, La) on bioactivity, structural and optical properties of these glasses. Unsoaked and soaked glasses in SBF were investigated using X-ray diffraction, FTIR and UV–vis spectroscopy.

## 2. Experimental

### 2.1. Preparation of the glasses

Glass compositions (mol.%) and their label are given in Table 1. The oxides were ball milled for 2 h in acetone medium

* Corresponding author. Tel.: +91 1752393130; fax: +91 1752393005.
*E-mail address:* kusingh@thapar.edu (K. Singh).

0272-8842/$36.00 
doi:10.1016/j.ceramint.2009.06.006

Table 1
Glass composition (mol.%) with their label.

| Sample Label | $SiO_2$ | CaO | $B_2O_3$ | $M_2O_3$ |
|---|---|---|---|---|
| GY | 40 | 30 | 20 | $10Y_2O_3$ |
| GA | 40 | 30 | 20 | $10Al_2O_3$ |
| GC | 40 | 30 | 20 | $10Cr_2O_3$ |
| GL | 40 | 30 | 20 | $10La_2O_3$ |

and melted in recrystallized alumina crucible at 1550 °C for 1 h to ensure complete mixing and homogenization. Finally, the melt was splat quenched over thick copper plates. Rectangular slices of glass were cut and polished using 600, 800 and 1200 grit silicon carbide.

### 2.2. Density and solubility measurement

The densities of soaked and unsoaked glasses were calculated using the Archimedes principle. Density data were used to calculate the molar volume ($V_m$), excess volume ($V_e$) and oxygen molar volume ($V_o$) of unsoaked glasses using the following equation.

$$\rho = \frac{w_a}{w_a - w_b} \times \rho_d \tag{1}$$

$M$ denotes the molar mass of the subjected glass.

$$V_e = V_m - \sum_i x_i V_m(i) \tag{2}$$

Here, $V_m(i)$ is the molar volume of each oxide constituent $x_i$ is the molar concentration of every oxide in the glass composition. Oxygen molar content in the glasses was calculated using Eq. (3). $M_i$ and $x_i$ is the molar weight of the oxide and oxygen content in the $i$th oxide.

$$V_o = \frac{\sum_i x_i M_i}{\rho \sum_i n_i x_i} \tag{3}$$

The solubility of the glass samples was calculated by the measurement of the weight loss in a SBF solution [13]. The durability measurement was done by dipping the glass sample in 100 ml of SBF solution and kept at 37 °C for different times.

### 2.3. X-ray diffraction (XRD)

All the glasses were examined by X-ray (XRD, Rigaku Geigerflex D/Mac at scanning speed $2^\circ\,min^{-1}$ and X-ray wavelength was 1.54 Å) to confirm the formation of hydroxyapatite on the glass surface after soaking in the SBF solution.

### 2.4. Band gap measurement

UV–vis absorption spectra were recorded at room temperature in the range 200–900 nm (Hitachi 330 UV-Visible absorption spectrophotometer, Japan). The absorption coefficient $\alpha(\nu)$ was calculated for each soaked and unsoaked sample at various incident photon energies, $h\nu$ by using the Lambert–Bear relation:

$$I = I_0\, e^{-\alpha t} \tag{4}$$

where $I_0$ and $I$ are the incident and transmitted photon intensity and $t$ is the sample thickness. The band gap $E_g$ was calculated by extrapolation of the linear region to meet $h\nu$ axis at $(\alpha h\nu)^2 = 0$ [14].

### 2.5. Fourier-transformation infrared (FTIR) spectroscopy

FTIR absorption spectra were recorded at room temperature in the range 400–4000 $cm^{-1}$ (Shimadzu, Japan, FTIR-8700). In the case of unsoaked sample, 4.0 mg powder of glass was mixed with 200 mg of KBr in an agate mortar and then pressed to obtain 13 mm diameter pellets for recording the absorption spectra. The FTIR analysis, after dipping in SBF, has also been performed on 13 mm diameter pellets prepared by mixing about 4 mg of materials scraped from the glass surface with KBr. For each sample, the spectrum represents an average of 20 scans, which were normalized to the spectrum of the blank KBr pellet.

## 3. Results and discussion

### 3.1. Density and solubility

The density of glasses was measured before and after soaking in SBF (Table 2). The GY glass sample exhibits higher density followed by GC, GL and GA. Interestingly, higher density samples show negative excess volume. It means these glasses exhibit more compactness with less porosity. In other words the higher density of these glasses can be explained on the basis of $Y_2O_3$ and $Cr_2O_3$ which eliminate vacancies inside the system by pushing them onto the surface [15–17]. Sample weight measurement provides a good estimation of dissolution. It is evident from Table 2 all the samples to show a weight loss >10% after 25 days immersion in SBF solution. Percent weight loss is highest for GA followed by GL. However, GY shows the lowest weight loss and exhibited good durability in SBF solution. Interestingly, $Y_2O_3$ containing glass exhibits higher density than other glasses. It may be attributed to the molar volume of GY glass lower than for other glasses. Moreover, this particular glass shows the $V_e$ value in negative which clearly indicates more compact structure than other glasses. On the

Table 2
Variation in density before and after dipping in SBF solution.

| | GY | GA | GC | GL |
|---|---|---|---|---|
| Density ($g/cm^3$) unsoaked | 3.93 | 2.27 | 3.32 | 2.52 |
| Density ($g/cm^3$) soaked | 4.01 | 1.30 | 3.66 | 1.21 |
| Weight loss (%) | 11.17 | 50.45 | 17.2 | 47.4 |
| Molar vol., $V_m$ ($cm^3$/mol) | 19.69 | 28.63 | 21.08 | 34.53 |
| Excess vol., $V_e$ | −5.00 | 5.87 | −2.04 | 9.32 |
| $O_2$ mol. vol., $V_o$ | 9.84 | 4.31 | 10.54 | 17.26 |
| Band gap (eV) unsoaked | 2.7 | 2.0 | 2.5 | 2.3 |
| Band gap (eV) soaked | 2.4 | 2.5 | 2.3 | 2.8 |

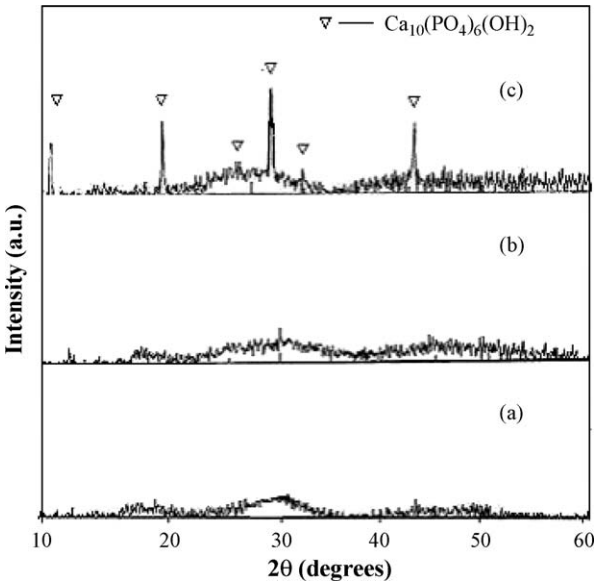


Fig. 1. XRD diffractogram for sample GY (a) 0 h, (b) 400 h and (c) 600 h.

other hand the least durable glass (GL) however, exhibits very high value of $V_e$ along with higher oxygen molar volume, $V_o$ as shown in Table 2. Interestingly, those samples which show higher dissolution rate could not form the crystalline hydroxyapatite layer even after 25 days soaking in SBF solution. This type of behaviour of these samples indicates that hydroxyapatite layer formation cannot be associated with high dissolution rate. It may depend upon some other factors such as surface reactivity, local environment of glass matrix and their affinity with SBF.

### 3.2. X-ray diffraction analysis

XRD pattern of as quenched silica based glasses possess the characteristic hump which is a clear manifestation of amorphous nature of the glasses. A typical XRD pattern of the as prepared GY glass system is shown in Fig. 1(a). After soaking for 17 days, a crystalline phase is formed on the surface of glass as shown in Fig. 1(b). As the soaking time increase from 17 to 25 days, the crystalline phase becomes more prominent. The XRD peaks were indexed using ICCD card no 74-0565. Similarly, GC samples also formed the crystalline HA layer after dipping in SBF as shown in Fig. 2(a) and (b). In this sample, XRD peaks are sharper than GY sample. The formation of hydroxyapatite layer might have started in early stage of soaking as compared to GY sample. However, in both the cases the crystalline HA layer could not grow fully on the surface of these samples. In case of GA and GL samples during initial stage of soaking the amorphous HA layer might have formed which later gets dissolved. These two samples also show very high rate of dissolution and reduced value of density after soaking in SBF. Similar results have also been observed in our earlier studies on bio-ceramic glasses [18]. The dissolution of $Ca^{2+}$ ions from the glass and phosphate ions from SBF solution plays an important role in the initial stage of apatite formation [19]. Basically dissolution of calcium ions from the glass

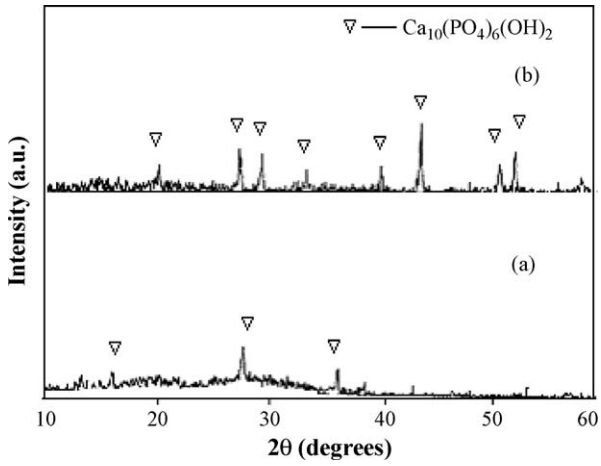


Fig. 2. XRD diffractogram for sample GC (a) 400 h and (b) 600 h.

increases the activity of apatite in the surrounding body fluids. The hydrated silica formed on the surface provides sites for apatite nucleation. Once the apatite nuclei are formed, they grow spontaneously by combining with calcium and phosphate ions from the surrounding fluid. High rate of dissolution of GA and GL bioglasses might be supersaturating the SBF solution in the early stage of soaking so that HA layer could not form on the glass surface.

### 3.3. Band gap investigations

The band gaps before dipping and after dipping samples are summarized in Table 2. Higher band gap is observed in GY samples as compared to other unsoaked samples. This observation can be attributed to the structural network difference brought by the replacement of different intermediate cations in these glasses. Glass GY exhibits higher $E_g$ than other glasses, hence corresponding to higher chemical durability. The decrease in $E_g$ for other glasses can be explained on the basis of lower average bond energy, which leads to decrease in the energy of the conduction band edge. The band gaps of GY and GC decrease after soaking these samples in (SBF) solution whereas, band gap increases in GA and GL glasses after dipping in SBF. The formation of crystalline hydroxyapatite layer on the surface of GY and GC sample reduces the porosity and increases ordering which lead to decrease in optical band gap. On the other hand, band gap of GA and GL exhibits the reverse trend than GY and GC samples. As shown in Table 2, these samples show higher weight loss with lower density and could not form apatite layer. It indicates that these samples became depleted due to higher rate of leaching. This leads to more disordering in these samples. Therefore, the band gap in GA and GL samples increases after immersion in simulated body fluid.

### 3.4. FTIR transmission spectra of soaked and unsoaked bioglasses

It was observed that FTIR spectra of soaked and parent bioglass had remarkable differences in the region between 750

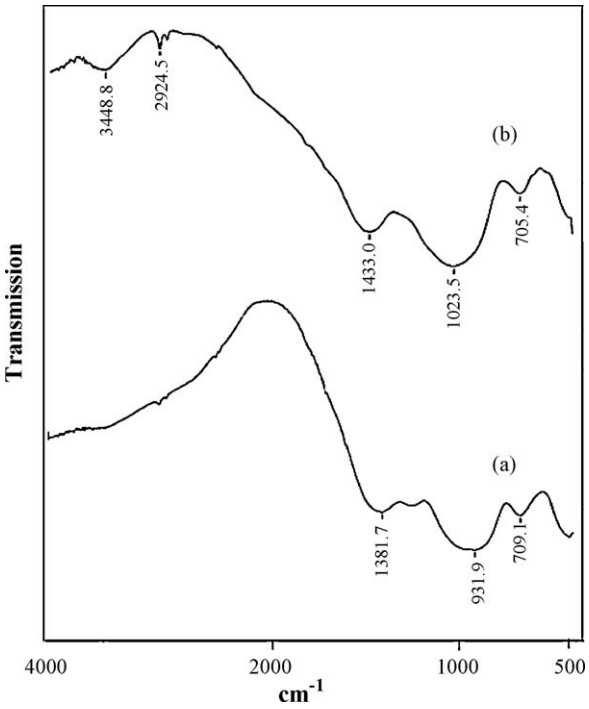


Fig. 3. FTIR spectra showing change in sample GY (a) 0 h and (b) 600 h.

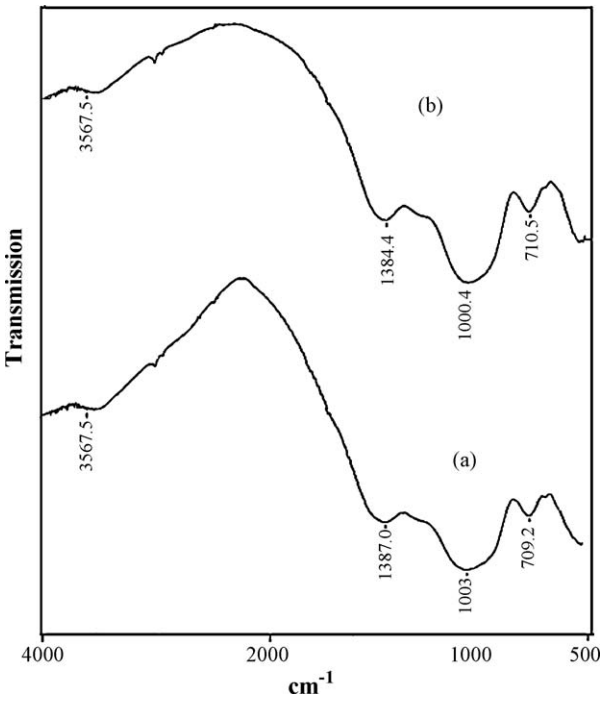


Fig. 4. FTIR spectra of sample GC (a) 0 h and (b) 600 h.

and 500 $cm^{-1}$. All dipped bioglass samples show new absorption bands in this region at (650–619 $cm^{-1}$) and (580–570 $cm^{-1}$) which can be attributed to the vibrational and rotational modes associated with calcium phosphate phase [20]. The weak reflection at 1620 $cm^{-1}$ can be assigned to the molecular water. The broad band centered at 3438 $cm^{-1}$ can be assigned to hydroxyl group (–OH) or silanol group (SiO–H). The glass sample GY after dipping in simulated body fluid (SBF) solution shows the broad hump ~3500 $cm^{-1}$ due to the $OH^-$ group. On the other hand, there is no peak at that region in sample GY before dipping in simulated body fluid (SBF) solution. There is another peak ~700 $cm^{-1}$ which again shows the presence of $OH^-$ ions as shown in Fig. 3. These results clearly indicate formation of the hydroxyapatite layer in sample GY after dipping in the simulated body fluid (SBF) solution. Interestingly, in GY and GC glasses after soaking in SBF exhibited a band at 1023 $cm^{-1}$ which indicates the formation of phosphate layer. Usually the band at 1025 $cm^{-1}$ assigned to P–O stretching [21], is superimposed over the bands relative to the Si–O–Si stretching mode and is not distinguishable. Therefore the sharpening of this band after soaking can be attributed to P–O stretching vibrations. In sample GC there is change in the peak around 3500 $cm^{-1}$ before and after dipping in solution as shown in Fig. 4(a) and (b). After dipping in SBF solution sample shows the broad hump ~3500 $cm^{-1}$ which is due to the $OH^-$ group as explained earlier and also the peak formation ~1470 $cm^{-1}$ can be correlated to carbonate group [22]. Thus the simultaneous presence of the above bands and decrease of intensity of $BO_3$ units (~709 $cm^{-1}$) confirms the formation of CaP hydroxyapatite layer and hence these glasses can be designated as biomaterials [23–25].

FTIR spectra of GA and GL samples could not show any appreciable change in transmission bands before and after dipping in SBF as shown in Fig. 5(a) and (b) and Fig. 6(a) and (b), respectively. The transmission bands at 800–1100 $cm^{-1}$ become sharper in GA sample after soaking in SBF solution. This indicates that a reaction does occur on the surface with the formation of a silica gel-like layer [26]. On the other hand,

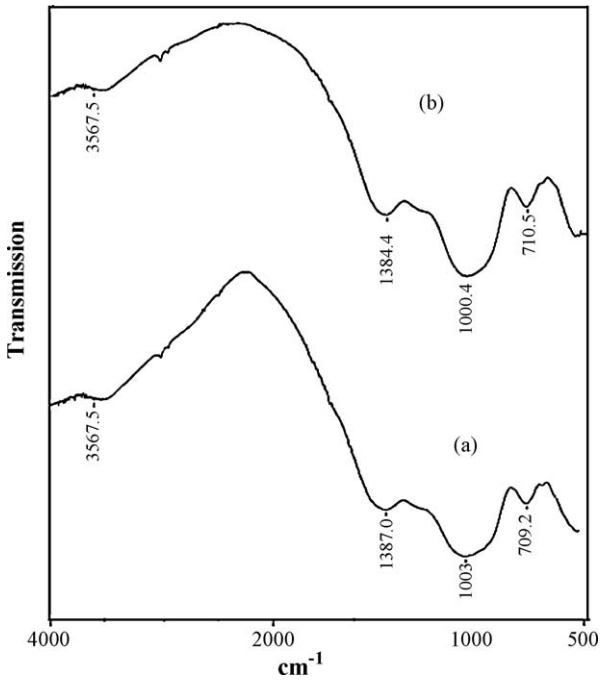


Fig. 5. FTIR spectra shows sample GA (a) 0 h and (b) 600 h.

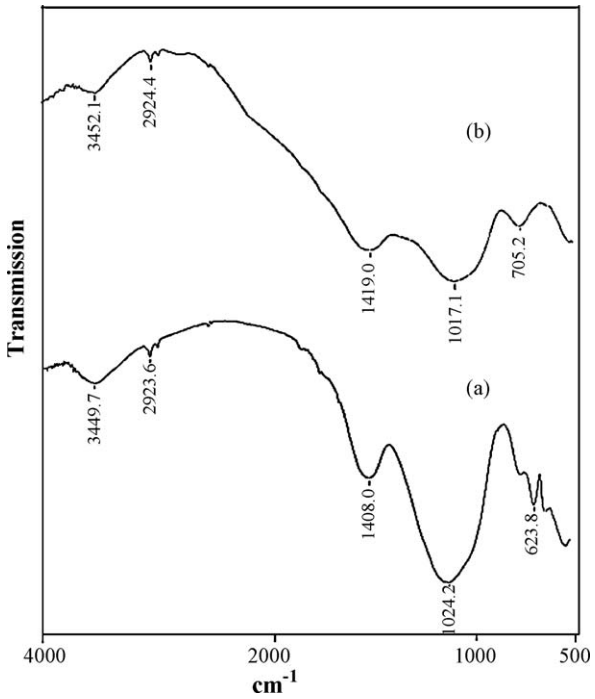


Fig. 6. FTIR spectra of sample GL (a) 0 h and (b) 600 h.

the GL sample exhibit broader FTIR spectra after soaking in SBF solution due to the presence of higher number of non-bridging oxygens and therefore the extension of the transmission band to lower frequencies. The density and oxygen molar volume, $V_o$ also indicates higher disordering and porosity in GL glasses.

## 4. Conclusions

In present investigation, the influence of the intermediate oxides was investigated on bioactivity and structural properties of calcium borosilicate glasses. The addition of $Y_2O_3$ and $Cr_2O_3$ increase the compactness of the glass matrix and leads to crystallization of hydroxyapatite layer during *in vitro* testing. $Al_2O_3$ and $La_2O_3$ containing glasses could not form the crystalline HA layer even after 25 days of soaking in SBF with decreasing band gap. However, these glasses exhibited higher rate of dissolution than GY and GC samples. The formation of HA layer depends upon many factors such as formation of silanol group, chemical nature of intermediate oxides and their field strength in glass matrix. It can be concluded that addition of intermediate oxides play an important role in determining the bioactive behaviour of the calcium borosilicate glasses.

## Acknowledgements

The authors gratefully acknowledge financial support from the Department of Science and Technology, India under the research grant SR/S2/CMP-48/2004. The authors also gratefully acknowledge Prof. O.P. Pandey, Head, School of Physics and Materials Science, Thapar University, Patiala for his support and helpful discussions.

## References

[1] L.L. Hench, Bioceramics: from concept to clinic, J. Am. Ceram. Soc. 749 (7) (1991) 1487–1510.
[2] T. Kokubo, S. Ito, Z.T. Hung, T. Hyashi, M. Shigimata, S. Saskka, T. Kitsugi, T. Yamamuka, Biomedical material template for in-vitro synthesis of bone tissue, J. Biomed. Mater. Res. 24 (1990) 331–340.
[3] Y. Ebisawa, T. Kokubo, K. Ohura, T. Yamamura, J. Mater. Sci.: Mater. Med. 1 (1990) 239.
[4] L.L. Hench, R.J. Splinter, W.C. Allen, T.K. Greenlee, Mechanism of interfacial bonding between ceramics and bone, J. Biomed. Mater. Res. Symp. 2 (1971) 117–141.
[5] T. Kokubo, CRC Handbook of Bioactive Glasses and Glass Ceramics, CRC Press, Boca Raton, FL, 1990.
[6] C. Oktsuki, T. Kokubo, K. Takatsuka, T. Yamamuro, Compositional dependence of bioactivity of glasses in the system $CaO–SiO_2–P_2O_5$ and in-vitro evaluation, Nippon Seramikkusu Kyokai Gakujustu Ronbunshi 99 (1991) 1–6.
[7] H.S. Ryu, J.K. Lee, J.H. Seo, H. Kim, K.S. Hong, D.J. Kim, J.H. Lee, D.H. Lee, B.S. Chang, C.K. Lee, S.S. Chung, Novel bioactive and biodegradable glass ceramics with high mechanical strength in the $CaO–SiO_2–B_2O_3$ system, J. Biomed. Mater. Res. 68 (2004) 79–89.
[8] N. Lahl, K. Singh, L. Singheiser, K. Hilpert, Crystallization kinetics in $AO–AbO_3–SiO_2–B_2O_3$ glasses, J. Mater. Sci. 35 (2000) 3089–3096.
[9] J.AI Haidary, M.Al. Haidari, S. Qrunfuleh, Effect of yttria addition on mechanical physical and biological properties of bioactive $MgO–SiO_2–P_2O_5–CaF_2$ glass ceramic, Biomed. Mater. 3 (2005) 15005–15010.
[10] V. Salih, A. Patel, J.C. Knowles, Zinc containing phosphate based glass for tissue engineering, Biomed. Mater. 2 (2007) 11–20.
[11] A. Wisbey, P.J. Gregson, M. Tuke, Application of PVD Tin coating to Co–Cr–Mo based surgical implants, Biomaterials 8 (6) (1987) 477–480.
[12] T. Schwickert, R. Sievering, P. Geasee, R. Conradt, Glass ceramic materials as sealants for SOFC applications, Mater.-wiss u. Werkstofftech. 33 (2002) 363–366.
[13] T. Kokubo, Hand Kushitani, S. Sakka, Solution able to reproduce in vivo surface structure changes in bioactive glass ceramics, J. Biomed. Mater. 24 (1990) 721–734.
[14] L.L. Hench, CRC Handbook of Bioactive Glasses and Glass Ceramics, CRC Press, Boca Raton, FL, 1990.
[15] T. Kokubo, Ito. Sand, S. Sakka, Formation of a high strength bio-active glass ceramic in the system $MgO–CaO–SiO_2–P_2O_5$, J. Mater. Sci. 1 (1982) 536–540.
[16] T. Kokubo, S. Ito, M. Shigematsu, S. Sakka, Fatigue and lifetime of bioactive glass–ceramic (A-W) containing apatite and wollastonite, J. Mater. Sci. 22 (1986) 4067–4070.
[17] T. Kasuga, Y. Kasugya, M.T. Uno, K. Nakajima, Preparation of zirconia toughened glass ceramic, J. Mater. Sci. 23 (1988) 2255–2258.
[18] K. Singh, D. Bahadur, Characterization of $SiO_2–Na_2O–Fe_2O_3–CaO–P_2O_3–B_2O_3$ glass–ceramic, J. Mater. Sci. Mater. Med. 10 (1999) 481–484.
[19] H. Kushitani, C. Ohtsuki, S. Sakka, T. Yamamura, Chemical reaction of bioactive glass and glass ceramics, J. Mater. Sci.: Mater. Med. 3 (1992) 79–83.
[20] K.A. Gross, L. Berzin, R. Cimdin, V. Grossb, Calcium phosphate bioceramics research in Latvia, Ceram. Int. 25 (1999) 231–237.
[21] Y. Kim, A.E. Clark, L.L. Hench, Early stages of calcium phosphate formation in bioglasses, J. Non Cryst. Solids 113 (1989) 195–202.
[22] H.A.El. Batal, M.A. Azooz, E.M.A. Khalil, A. Monem Soltan, Y.M. Hamdy, Compositional dependence of calcium phosphate larger formation in fluoride to bioglasses, Mater. Chem. Phys. 80 (2003) 599–609.

[23] J.M. Olivera, R.N. Correia, M.H. Fernandes, Effect of Si-specification on the in vitro bioactivity of glasses, Biomaterials 23 (3) (2002) 71–79.
[24] Manupriya, K.S. Thind, G. Sharma, K. Singh, V. Rajendran, S. Aravindan, Soluble borate glasses: in vitro analysis, J. Am. Ceram. Soc. 90 (2) (2006) 467–471.
[25] C.V. Ragel, M. Vallet-Regi, L.M. Rodriguez-Lorenzo, Preparation and in vitro bioactivity of hydroxyapatite/solgel glass biphasic material, Biomaterials 23 (2002) 1865–1872.
[26] F. Branda, F. Acrobello-Varlese, A. Costantini, G. Luciani, Effect of substitution of $M_2O_3$ (M = La, Y, In, Ga, Al) for CaO on the bioactivity of 2.5 $CaO{\cdot}2SiO_2$ glass, Biomaterials 23 (2002) 711–716.